Soft Matter

Cite this: *Soft Matter*, 2012, **8**, 3762

www.rsc.org/softmatter

PAPER

A novel methodology for systematic study on molecular release from microscale reservoirs†

Dong Choon Hyun, Bongsoo Kim, ChooJin Park and Unyong Jeong*

Received 13th December 2011, Accepted 16th January 2012
DOI: 10.1039/c2sm07355b

We have developed a novel method to systematically investigate molecular release. A series of processes including buckling of thin polymer films, deposition of solute molecules, and transfer to other substrates enabled the fabrication of uniform and submicron-sized tunnel-like molecular reservoirs. From the release profiles, diffusivity and solubility of the solute molecules in the polymeric barriers were calculated. As a model study, we investigated the release of rhodamine B and FITC-labeled dextran polymer representing small molecules and large molecules. The degree of hydration of the polymer barrier was controlled by changing the chain end group of polystyrene (PS) by *tert*-butyl (PS-*t*-Bu) and nitrilotriacetic acid (PS-NTA). The NTA-terminated PS thin films showed 13% water uptake regardless of the film thickness while the bare PS and PS-*t*-Bu barriers exhibited 4% and 6% uptake. This difference in hydration affected release behavior of the molecules. The release of small molecules was dependent on the barrier polymers, while the release of large molecules was completely blocked due to the restricted chain movement of the barrier polymers. Surface treatment by CF_4 plasma on the PS-NTA barriers considerably retarded the release of small molecules and blocked the release of large molecules. The release behavior could be well explained by the diffusivity and solubility calculated from the release profile.

1. Introduction

Diffusion and transport of molecules in polymer layers are of great importance in polymeric coating, tackification, ionically conducting polymers, and controlled drug release.[1] In particular, molecular release through the polymer layers in a controlled or pre-designed manner has been attracting enormous interest because the release control can provide immediate applications in drug delivery, cosmetics, smart capsules, paintings, *etc.*[2–5]

Based on physical and chemical characteristics of membrane polymers, there are three primary mechanisms in molecular release through the polymer layers: diffusion, degradation, and swelling followed by diffusion.[6] Diffusion is commonly involved in the three mechanisms. Diffusion of molecules in the polymer layer takes place on a macroscopic scale through the membrane with macropores[7] or on a molecular level through the excluded volume between the polymer chains.[8] Penetration of the molecules from the reservoir through the polymer barrier is primarily dependent on the solubility and diffusivity of the molecules in the polymer layer. In the release of the molecules, the polymer layer first uptakes a solution medium, and the molecules are mixed in the polymer layer and diffuse out to the solution medium. Therefore, the release rate of the molecules is affected by the solubility and diffusivity of the molecules in the swollen polymer layer as well as by the surface energy and thickness of the polymer barrier. The surface energy of the membrane can considerably affect the degree of swelling. In addition, the diffusivity of the molecules is influenced by the relative size of pores or channels in the polymer layer compared with the size of solute molecules. The mobility of large molecules should be sensitive to the molecular weight of the membrane polymers.

Even though many studies have been carried out over the controlled release, still the factors affecting the release have been poorly understood. This is mainly due to the lack of methodology by which the various factors can be systematically controlled. Most studies on the release have been done case-by-case with colloids, fibers, and large sized membranes. The release control has been carried out by changing the structure of colloids, crosslinking, surface treatment, and molecular weight of diffusion barriers.[9] However, such studies cannot provide quantitative comparison for the relative effect between the controllable factors. And the diffusivity and solubility of the molecules in the membrane are not readily obtainable. This report is aimed at suggesting a method allowing a systematic study on molecular release through polymer thin layers.

Since most controlled release systems are in the micron or submicron scale, we developed a microscale reservoir system. The reservoir is covered with a polymer thin layer and includes target molecules. It is difficult to fabricate a microscale reservoir

Department of Materials and Science, Yonsei University, 134 Shinchon-dong, Seoul, Korea. E-mail: ujeong@yonsei.ac.kr

† Electronic supplementary information (ESI) available: The optical microscope images, SEM images, and AFM images showing the reversible buckling and transfer. See DOI: 10.1039/c2sm07355b

by a simple coating and covering process. Spin-coating a solute molecule is only possible with high-molecular-weight solute molecules. It is difficult to spin-coat small molecules in a uniform dimension. The other way is to drop a solution on a substrate, but the final drop size of the solutes should be much larger than the microscale. In addition, the reservoir in our study contains vacancy, which resembles the structure of micelles. A similar approach with a solid substrate with negative micropatterns is possible, but the selective deposition of the solute molecules in the empty room needs elaborate efforts.

In this study, the diffusion-controlled release from the reservoir was analyzed with a simple model[10] and quantitatively obtained the diffusivity and solubility of the molecules in the polymer barrier. Scheme 1 illustrates the experimental process in this study: (1) buckling of a polymer thin layer on a plasma-treated PDMS elastomer, (2) loading of an active agent on the buckled surface by spin-coating, (3) transfer of the buckled polymer layer to another substrate, and (4) release test through the polymer layer. Buckling is a topological structure which is frequently found in nature. Buckling takes place when the top layer on the elastomer substrate has much higher Young's modulus than the elastomer.[11] The mismatch in thermal expansion or elastic modulus between two layers induces compressive stress. The stress relaxation creates a regular wavy pattern with a fixed wavelength and magnitude. The structure has been mainly used in flexible electronics and devices[12] and modern metrology[13] in academy. Recently we reported a release system using the buckled polymer film that could respond to mechanical strains.[14] The sinusoidal nature of the buckling pattern helps a selective deposition of the molecules in the troughs of the buckling patterns during spin-coating or dip-coating.[14,15] After the selective deposition of the molecules, the whole buckled polymer layer can be transferred to another substrate when the adhesion

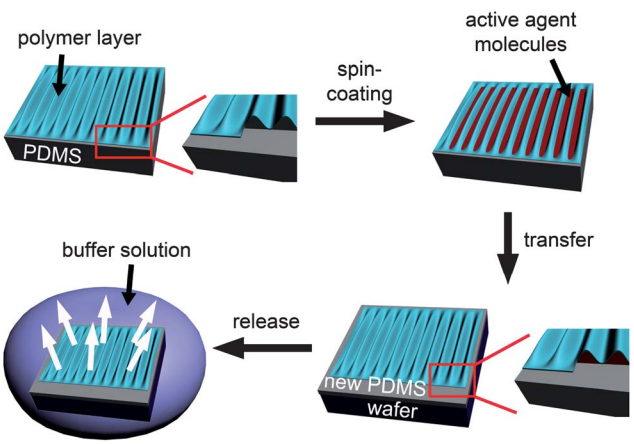

Scheme 1 Schematic illustration demonstrating the fabrication process of the molecular reservoirs covered with polymer thin layers. Thermal heating and subsequent cooling of a polymer-coated PDMS elastomer substrate generate a buckling pattern. Active molecules are selectively deposited in the trenches of the buckling pattern by simple spin-coating. The buckled polymer thin films are transferred to a new substrate, a PDMS-coated Si wafer. The active agent molecules are entrapped in the long microtunnels with closed ends, like a collection of greenhouses. The active agent molecules are released through the polymer barrier into a buffer solution.

between the polymer layer and the new substrate is stronger than that between the polymer layer and the PDMS substrate. We used a PDMS-coated Si wafer as the new substrate. The thickness of the PDMS coating layer was 10 μm. Because the wafer is impermeable, material diffusion is only allowed through the transferred polymer layer. In order to enhance the transfer of the buckled polymer layer, the buckled surface was dipped in water before the deposition of the molecules in the trough. Because the PDMS substrate had been plasma-treated for polymer coating, water infiltrated in the interface between the polymer layer and the hydrophilic oxidized layer, which lowered the adhesion and allowed the transfer of the buckled layer to the substrate.[13a,c] The transferred buckling layer makes tunnels with closed ends, like greenhouses, so that water cannot dissolve the molecules during the transfer process.

The above process is advantageous in that we can readily change the parameters in molecular diffusion: (i) chemical and physical property of the polymer layer, (ii) variation in membrane thickness, (iii) loading of various active agents, and (iv) surface treatment of the polymer layer. Further, the diffusivity and solubility of the molecules can be readily obtained according to the adjusted parameters. This study will be beneficial to analyze diffusion behavior of molecules, thus to design a controlled release system for specific target drugs.

2. Experimental

Materials

Poly(styrene) (PS, M_w = 20 000) was polymerized by anion polymerization. The polydispersity index (PDI) was 1.05. PS (M_w = 1 000 000) was purchased from Aldrich. Polystyrene with a *tert*-butyl ester end group (PS-*t*-Bu, M_n = 18 000, PDI = 1.06) was synthesized by atom transfer radical polymerization and the *t*-Bu group was transformed into nitrilotriacetic acid (NTA) to form PS-NTA (M_n = 15 000, PDI = 1.22) following the previous procedure.[16] The Sylgard 184 elastomer kit from Dow Corning was used to make the poly(dimethylsiloxane) (PDMS) substrate and thin film. Rhodamine B and FITC-labelled dextran (M_w = 10 000) were purchased from Aldrich.

Sample preparation

Flat PDMS substrates were prepared by mixing the siloxane prepolymer and its crosslinker at 20 : 1 ratio (w/w). The mixtures were hosted in glass Petri dishes (10 cm in diameter). They were left at room temperature to allow the trapped air bubbles to escape and then cured at 80 °C for 24 h. Small substrates with dimensions of 3 cm × 3 cm were cut from the cured PDMS elastomers and placed on clean glass slides. The PDMS substrates were exposed to oxygen plasma (Cute-100LF, Femto Science Inc., Korea) of 40 W with a flow rate of 22 sccm and at a base pressure of 0.945 Torr for 40 s. Polymers were dissolved in toluene and spin-coated on the PDMS substrates at 3000 rpm for 30 s. The polymer-coated PDMS substrates were annealed in a preheated vacuum oven (180 °C) for 1 h and taken out from the oven. They were cooled to room temperature in the air. The isotropic compression created by the difference in thermal expansion of the polymer and the PDMS substrate generated disordered buckling. The thickness of the polymer layers on the

PDMS substrate was controlled by adjusting the polymer concentration. The specimen was dipped in DI water for 20 min and then dried in a vacuum for 12 h. This process was for decreasing the adhesion between the buckled polymer layer and the PDMS substrate to help the transfer of the buckled layer to a new substrate. The buckled surfaces were exposed to oxygen plasma (30 W, 22 sccm, 0.945 Torr, 30 seconds) to change the surface hydrophilicity. Rhodamine B solution (0.5 wt%) in ethanol and FITC-labelled dextran solution (0.25 wt%) in an aqueous solution (ethanol/water, 1 : 4, v/v) were spin-coated on the buckled patterns to selectively deposit the target molecules in the troughs of the patterns. After depositing the molecules by spin-coating, the specimens were dried in a vacuum for 3 h and then brought into contact with a PDMS-coated Si wafer. For the PDMS coating on a Si wafer, a mixture of the siloxane prepolymer and its crosslinker (40 : 1, w/w) was spin-coated at 5000 rpm for 3 min. After degassing, it was cured at 80 °C for 24 h. The molecule-containing buckled substrates were contacted with the new substrate. After 5 min, the substrates were peeled off. The buckling layer was transferred to the new substrate. In order to investigate the effect of surface hydrophilicity, the polymer surface was modified with CF_4 plasma treatment which was conducted at 30 W with a flow rate of 15 sccm for 3 min.

Release test of the molecules

The samples were immersed in a PBS buffer solution (500 mL in a vial) at pH 7 for the release test. The cap of the vial was tightly sealed to prevent evaporation of the buffer solution during the test. The buffer solution was kept at 25 °C and mechanical shaking was applied to maintain the sink condition during release. The samples were taken out of the buffer solution. Intensity change of the active agent loaded in the sample was analyzed by using an optical microscope and a software (analySIS LS Starter). The optical microscope images were of the same magnification (×500) on identical areas of the specimens. The samples were then placed back to the buffer solution. Photobleaching was negligible in this study, causing less than 0.1% error.

Measurement of water absorption in polymer thin films

In order to investigate the water uptake in polymer thin films, we monitored their weight and thickness. The polymer thin films with four thicknesses (80 nm, 110 nm, 200 nm, and 240 nm) were spin-coated on a 4 inch Si wafer. In the gravimetric measurement, thermal annealing was conducted at 180 °C for 1 h in a vacuum oven. The thin films were put in a puddle of water for a scheduled time. For each measurement, the puddle of water was completely removed using a syringe and clean papers. The process was conducted under humid conditions to prevent undesired evaporation of water. The amount of uptake was quickly measured using a microbalance (Mettler Toledo, XS105) with precision ~0.01 mg. For the measurement of the degree of swelling, freeze-drying was employed. The spin-coated polymer films were immersed in water and then quenched with liquid nitrogen. After keeping the films in a vacuum for 48 h, the thicknesses were estimated with a spectroscopic reflectometer (ST2000-DLXn, K-mac Co.).

Instruments

The thickness of polymer thin films was measured by a spectroscopic reflectometer. The buckled surface was analyzed by an atomic force microscope (AFM, Dimension 3100, Digital Instrument Co.) and a scanning electron microscope (SEM, S-4300, Hitachi Co.).

3. Results and discussions

Fabrication of a tunnel-like reservoir covered by polymer thin films

Fig. 1A and B show AFM images of the PS buckling pattern on the PDMS substrate (A) and its transferred pattern (B) to the new substrate. The large hydrophobic character of the PDMS substrates forced organic solutions to dewet during spin coating.[17] Short-time exposure to oxygen plasma created a hydrophilic oxidized layer on the surface and helped uniform spin-coating on the PDMS substrate.[18] The film thickness in Fig. 1 was 110 nm. The sample was heated at 180 °C and then cooled down to room temperature. The thermal heating and cooling generated a sinusoidal wavy buckling pattern with 6.01 ± 0.39 μm wavelength and 785 ± 37 nm magnitude as shown in Fig. 1A. The wavelength and magnitude of the buckling pattern can be tuned by the elastic modulus and thickness of the polymer layer.[19] The buckling pattern on the PDMS substrate was dipped in DI water, taken out, and dried in a vacuum. They were flipped over and placed on a PDMS-coated Si wafer, making a conformal contact. The transfer of the buckling pattern was completed by peeling off the PDMS substrate, as shown in Fig. 1B. The transferred buckling pattern showed no change in the pattern features from the original one. No polymer remnant was found on the surface of the PDMS substrate. The successful

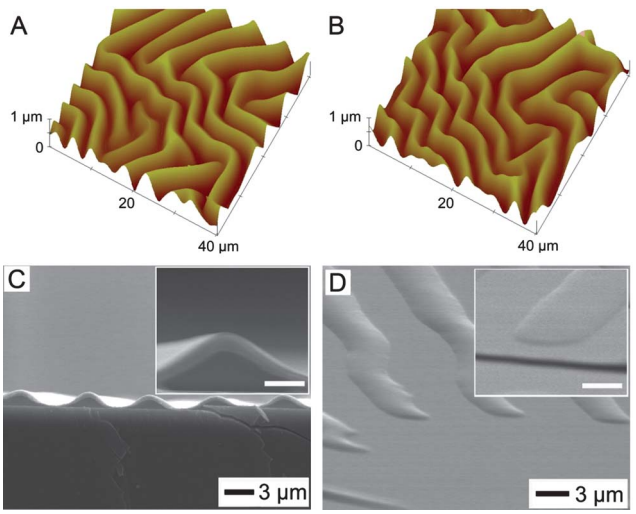

Fig. 1 (A) AFM image of a buckling pattern. (B) AFM image of the transferred pattern to the new substrate. The images demonstrate that the structure of the buckling pattern is maintained after the transfer. (C) SEM image of the hollow structure of the transferred pattern. The image was obtained by cracking the sample in liquid nitrogen. The inset is a closer look of the cross-section. (D) SEM image showing the ends of the transferred channels with closed ends. The inset is a closer look of an end. The scale bars in (C) and (D) are 1 μm.

transfer is attributed to the water infiltration through the interface between the hydrophilic oxidized surface of the PDMS substrate and the polymer film, thereby reducing the adhesion of the interface. In addition, usage of the stickier PDMS (40 : 1, w/w) on a Si wafer provided the stronger adhesion. The transferred patterns were hollow as shown in the cross-sectional SEM image of Fig. 1C. The sample for SEM was prepared by breaking the film in liquid nitrogen. A magnified image in the inset verifies the formation of the hollow channel. SEM images in Fig. 1D and its inset show the edges of the transferred buckling pattern where the channel ends were closed. This is because of an edge effect by which the compressive force decreases to zero at the substrate edge where a flat region without the buckling exists.[20] The hollow ridge with closed ends forms a long tunnel-like reservoir, like a long greenhouse, in which the target molecules can be stored. We can control the release of the molecules by changing the thickness and physical properties of the polymer layers which act as diffusion barriers.

Rhodamine B and FITC-labeled dextran were used as the model molecules representing low-molecular-weight drugs and high-molecular-weight drugs, respectively. Because the buckled polymer layer is hydrophobic, the surface was lightly exposed to oxygen plasma. The enhanced water contact to the surface helped deposition of the molecules *via* spin-coating. Optical microscope (OM) images in Fig. 2 show loading of the molecules that were selectively deposited in the troughs of the buckling patterns (Fig. 2A for rhodamine B and Fig. 2C for dextran). The blue stripes are the troughs and the lighter green stripes are the ridges. Fluorescent OM images in Fig. 2B and D demonstrate that the fluorescent lines exactly correspond to the troughs, exhibiting that the molecules were evenly deposited in the troughs with good homogeneity. Fig. 3 shows the SEM images (A and C) of the buckled patterns transferred to the new substrate. Comparison of the SEM images with the fluorescence microscope images (B and D) indicates that the solute molecules

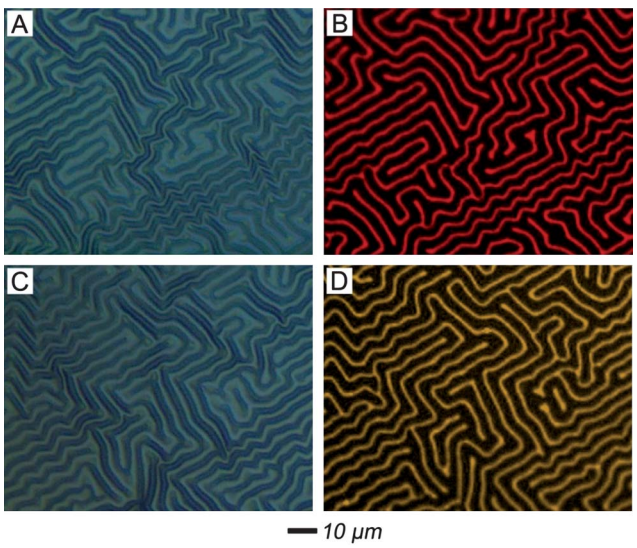

Fig. 2 Optical microscope images (A and C) and fluorescence optical microscope images (B and D) showing the selective deposition of the molecules in the troughs of the buckling pattern by spin-coating. (A and B) Rhodamine B; (C and D) FITC-labeled dextran.

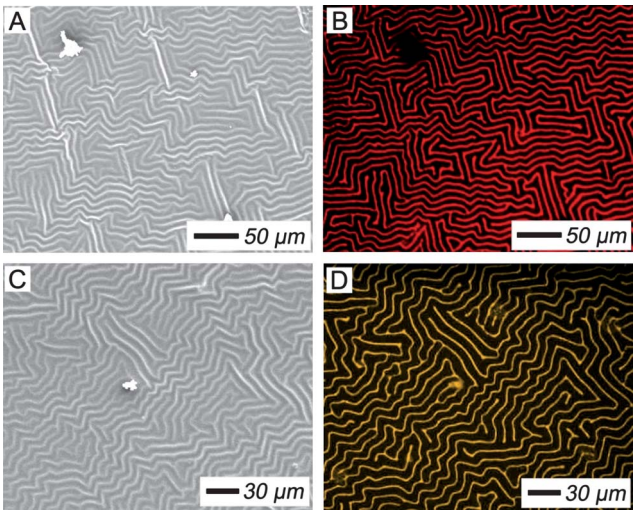

Fig. 3 SEM (A and C) and the corresponding fluorescence optical microscope (B and D) images of the pattern transferred to the new substrates. (A and B) Rhodamine B; (C and D) fluorescent dextran. The images verify that the loaded molecules in the trough of the initial buckling pattern were placed inside the tunnels of the transferred patterns.

were placed below the ridge of each transferred pattern. This suggests that the transfer of the buckled thin layer can facilitate successful fabrication of a reservoir covered with a polymer diffusion barrier.

Determination of diffusivity and relative solubility in polymer layers

According to the proposed release mechanism in the membrane-controlled release systems,[8b] the solute molecules initially placed in the reservoir start to diffuse out through the polymer membrane, and then partition into the elution medium surrounding the membrane. A hydrodynamic diffusion layer and stagnant solution layer are also present at the surface of the system (see Fig. 4 for the diffusion layer scheme). The solute molecules diffuse by natural convection under a concentration gradient in the stagnant solution layer. The cumulative amount (Q) of the solute molecules released from the polymer membrane can be described by the following expression,

$$Q = A\left(\frac{C_p K D_d D_m}{K D_d h_m + D_m h_d} t - \frac{D_m D_d}{K D_d h_m + D_m h_d} \int C_{b(t)} dt\right) \quad (1)$$

where A is the surface area of the membrane and K is the partition coefficient defined as C_s/C_p. C_p and C_s are the concentration (solubility) of the solute molecules in the polymer layer (membrane) and solution (elution medium), respectively. D_m is the diffusivity in the membrane with a thickness (h_m) and D_d is the diffusivity in the hydrodynamic diffusion layer with a thickness (h_d). $C_{b(t)}$ is the concentration of the solute molecules at the interface between the diffusion layer and the bulk solution. Since the samples in this study are immersed in a large amount of buffer solution (500 mL) under mild mechanical shaking, $C_{b(t)}$ can be regarded to be 0. When the sink condition is maintained over the release, *i.e.*, $C_{b(t)} \approx 0$ or $C_s \gg C_{b(t)}$, eqn (1) can be reduced as follows.

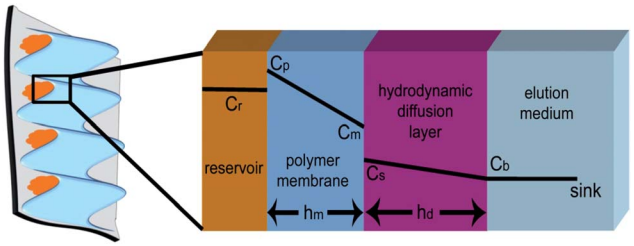

Fig. 4 Schematic diagram illustrating the concentration profile in a reservoir system using the transferred buckling membrane. The letter '*C*' represents the concentration of the solute molecules in the reservoir (C_r), in the polymer membrane (C_p), at the membrane/solution interface (C_m), at the beginning of the diffusion layer (C_s), and in the bulk of elution solution (C_b). Here C_p indicates the solubility of the molecules in the membrane. h_m and h_d are the thickness of the membrane and the hydrodynamic diffusion layer.

$$Q = A\left(\frac{C_p K D_d D_m}{K D_d h_m + D_m h_d} t\right) \quad (2)$$

Eqn (2) demonstrates that release of the molecules should have a constant release profile with time. Because the KD_dh_m term is significantly larger than the D_mh_d term in most diffusion barrier systems, the equation can be further simplified to

$$\frac{Q}{t} = \frac{AC_pD_m}{h_m} \quad (3)$$

This mathematical expression is based on the pseudo-steady state approximation, which means that the concentration gradient is linear across the membrane by following Fick's 1st law. However, it takes some time for a freshly prepared reservoir system to achieve the linear gradient, which calls a time lag. For a freshly made membrane without loaded molecules, a modified equation considering Fick's 2nd law is given by[21]

$$Q = \frac{AD_mC_p}{h_m}\left[t - \frac{h_m^2}{6D_m}\right] - \frac{2h_mAD_mC_p}{\pi^2}\sum_{n=1}^{\infty}\frac{(-1)^n}{n^2}e^{-n^2\pi^2D_mt/h_m} \quad (4)$$

As time goes to the steady state, eqn (4) has a form of

$$Q = \frac{AD_mC_p}{h_m}\left[t - \frac{h_m^2}{6D_m}\right] \quad (5)$$

In this study, the solutes are located in the long tunnel-like reservoir covered with a thin polymer layer. Eqn (5) can be applied to describe the release of solute molecules through a polymer thin layer while the solute concentration in the reservoir is much higher than the concentration in the polymer layer. Once the concentration of the molecules in the reservoir is significantly decreased so that the concentration gradient within the polymer layer starts to be lowered, the release profile begins to deviate from the linear relationship and the release rate slows down.

Eqn (5) reveals that the solubility (C_p) and diffusivity (D_m) of solute molecules in a polymer layer are controllable parameters of the release behavior. Even though the surface area (A) also can be an adjustable factor over the release, the measured dimensions in this study showed very small differences regardless of the polymer species and thickness. Therefore, it is reasonable that the surface area term results in negligible contribution to the difference in release characteristics. Then, the diffusivity (D_m) of solute molecules through a polymer layer can be determined from the relationship,[22]

$$D_m = \frac{h_m^2}{6t_l} \quad (6)$$

where t_l is the positive intercept at the time axis by extrapolation through the steady-state region (see Fig. S1 in the ESI†).

Water absorption in the polymer thin layers

The release of hydrophilic solute molecules should be governed by the degree of water absorption. We compared the water uptake of the thin films according to the chain end groups, molecular weight, and film thickness (80 nm, 110 nm, 200 nm, and 240 nm). The three hydrophilic carboxyl acid end groups of PS-NTA can promote hydration in the thin films. Compared with bare PS films, the PS-*t*-Bu thin films are expected to have a higher degree of water absorption because the large *tert*-butyl end group increases the free volume of the polymer chains and the existence of the carbonyl group slightly enhances affinity to water molecules.

Fig. 5A shows the kinetics of weight changes by the water absorption of the polymer thin films. The amount of uptake was quickly measured using a microbalance (Mettler Toledo, XS105) with precision ~0.01 mg. The weight change (M/M_0) for the PS-NTA thin film (1) was 1.13 regardless of the film thickness, which indicates 13% increase due to the water uptake. The weight increase was completed within 2 min. Plasma treatment has been widely employed to modify the surface property of the polymer films. When the PS-NTA thin films were treated with CF_4 plasma, the kinetics of the weight change was much sluggish although the final weight increase was the same, 13%. Complete water uptake of the plasma-treated film took 15 min. This is attributed to the hydrophobic fluorinated surface preventing the water absorption. The weight change of the PS-*t*-Bu layers and PS(20k) layers was 1.06 (6% increase) and 1.04 (4% increase), respectively. It is noticeable that water diffusion of the PS film was fast so that water uptake of the 240 nm PS film was completed within 10 min. This fast diffusion of water molecules in the PS thin film was already reported by previous research.[23] The final weight change was the same at any film thickness (Fig. 5B). And the degree of water uptake turned out to be independent of the molecular weight of PS chains. The thin films of PS(20k) and PS(1000k) showed the same weight change. As shown in Fig. 5A, the normalized weight of water uptake during the initial stage of diffusion is linearly proportional to the square root of the diffusion time, which indicates the water uptake followed Fick's law. The slope of the linear region at the initial stage allowed estimation of water diffusivity in the polymer thin films.[21] Regardless of the film thickness, the values were 1.24×10^{-12}, 1.61×10^{-12}, 1.97×10^{-12}, 8.03×10^{-13} and 8.69×10^{-12} $cm^2\ s^{-1}$ for PS(1000k), PS(20k), PS-*t*-Bu, CF_4 plasma-treated PS-NTA, and bare PS-NTA, respectively.

The water absorption in the polymer thin films was also verified by measuring the degree of swelling (Fig. 5C). Free-drying was employed for the measurement. The spin-coated polymer films were immersed in the water and then quenched with liquid

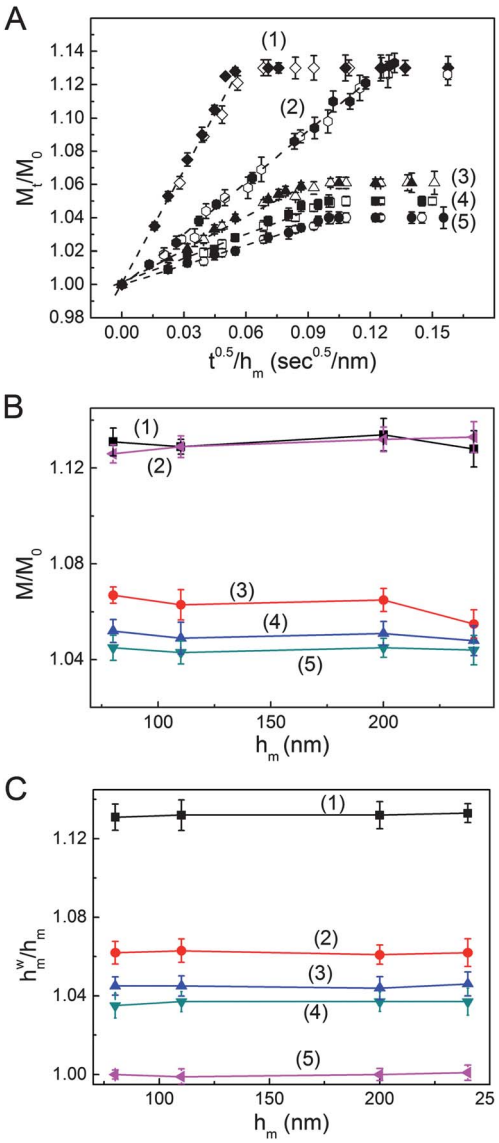

Fig. 5 (A) Time-dependent weight changes (M/M_0) of the polymer thin films by water uptake (open symbols: 110 nm, solid symbols: 240 nm). The dashed lines indicate Fickian fits. Each number in the plots denotes (1) PS-NTA, (2) CF_4 plasma-treated PS-NTA, (3) PS-*t*-Bu, (4) PS(20k), and (5) PS(1000k). (B) Weight changes of the polymer films with various thicknesses by water uptake (80, 110, 200 and 240 nm). Solid lines are guides to eyes. (C) Changes in thickness of the polymer films with various thicknesses by water uptake: (1) PS-NTA, (2) CF_4 plasma-treated PS-NTA, (3) PS-*t*-Bu, (4) PS(20k), and (5) PS(1000k). Solid lines are guides to eyes.

nitrogen. They were put in a vacuum oven at room temperature for 48 h. The thicknesses were estimated with a reflectometer. The thickness changes (h_m^w/h_m) were 1.037, 1.045, 1.062, 1.131, and 1.132 for PS(1000k), PS(20k), PS-*t*-Bu, CF_4 plasma-treated PS-NTA, and bare PS-NTA, in the order. h_m^w is the thickness after freeze-drying. The values were in good agreement with the results obtained by the weight increase.

Release of molecules through the polymer thin layers

For a systematic study on the release behavior, we varied the end group of PS, the thickness of the polymer layer (80 nm, 110 nm, 200 nm, and 240 nm), and the molecular size of solutes. Fig. 6 shows the release behavior of rhodamine B through polymer layers. The plots in Fig. 6 are the changes in fluorescence intensity *versus* the release time. It was normalized by the initial fluorescence before the release was allowed. Reduction in the intensity represents the release of the rhodamine molecules through the polymer layer: (A) PS(20k), (B) PS-*t*-Bu, and (C) PS-NTA. The dye molecules showed slow release at the initial stage. Such a time lag was observed ranging from 2 min to 1 h depending on the thickness of the polymer layer and the end group of the polymer chains. This is because the time is required for water uptake in the polymer layer as well as the outward diffusion of the molecules. After the initial time lag, the release exhibited a linear profile and then finally reached a plateau value (see Fig. S2 in the ESI† for long-time release profiles of rhodamine B). We took the time lag and the linear region to obtain diffusivity and solubility of the dye molecules from eqn (5) and (6). The linear relationship over time represents a steady-state release as a typical characteristic that is normally observed in the membrane-controlled release systems.[10] The release was retarded as the film thickness increased. Release of rhodamine B was the fastest in the PS-NTA layer and the slowest in the PS(20k) layer. 100% release was observed after 4 h in the 80 nm thick PS-NTA layer. Even in 240 nm thick layers, complete release was accomplished in 24 h. In contrast, the 80 nm thick PS(20k) layer allowed 13% release in 2 h and complete release was reached in 48 h (see the ESI†). The release through the 240 nm thick PS(20k) layer was largely slowed down, approaching the complete release in 120 h (see the ESI†). Fig. 6D summarizes the slopes in the steady-state region. The slope indicates the release rate of the dye molecules which was inversely proportional to the film thickness for all polymer membranes as expressed by eqn (5). The release rate in the PS-NTA layer was steepest compared with those of the PS(20k) and PS-*t*-Bu layers. The measured release rates in

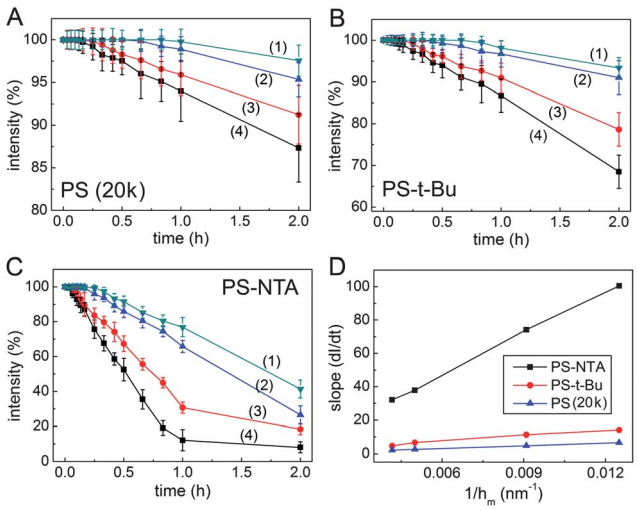

Fig. 6 Release behavior of rhodamine B through the various polymer membranes with different thicknesses: (A) PS(20k), (B) PS-*t*-Bu, and (C) PS-NTA. The slope (d*I*/d*t*) in the linear region of each plot indicates the release rate. The numbers in each plot correspond to the membrane thickness: (1) 240 nm, (2) 200 nm, (3) 110 nm, and (4) 80 nm, respectively. (D) The effect of polymer membrane thickness on release rates of rhodamine B. The solid lines are simple guides to eyes.

the PS-NTA layer were 100.53, 74.23, 37.89, and 32.15 (%/h) for thicknesses of 80 nm, 110 nm, 200 nm, and 240 nm, in the order. The values in PS-NTA were approximately 7-fold and 15-fold higher than PS-*t*-Bu and PS(20k), respectively.

It is noticeable that ethanol penetrates in the polymer film, promoting the possible loading of rhodamine in the polymer film. Long time dipping of the polymer films in the ethanol solution loaded a considerable amount of rhodamine, which caused a burst release at the early release stage. However, the amount of the diffused molecules for a short spin-coating time (30 s) was found negligible so that it did not make a considerable influence on the analysis. In the release test, the reservoir had a time lag before release. It proves the negligible effect of the molecular loading by the coating process. In addition, when we occasionally had samples with a crack or tearing, we observed fast release regardless of the thickness of the polymer membranes and polymer species. We never found incomplete capping at the ends of the channels, which means no burst release was found once if there were no cracks in the polymer membrane.

Fig. 7A shows the calculated diffusivity of rhodamine B in the polymer layers. The diffusivity was independent of the thickness of the polymer layers. The average values were 9.53×10^{-14}, 4.21×10^{-14} and 2.98×10^{-14} $cm^2\ s^{-1}$ for PS-NTA, PS-*t*-Bu, and PS(20k), in the order. This dependence of diffusivity on the polymer species had been researched for a long time. Zentner *et al.* investigated the diffusivity of progesterone in various biomedical polymers and copolymers having different compositions.[24] Zhao *et al.* simulated the diffusivity of aspirin in amorphous polymers.[25] Diffusion of molecules in a polymer matrix is considered as two mechanisms: (1) motion within free volumes (cavities) and (2) movement of free volumes originating from the wriggling of the polymer chain. The former is controlled by the size of the free volume in the polymer and the latter is strongly affected by the segmental motion of the polymer chains. In previous studies, the diffusion behavior of small molecules in the polymer could be controlled by the free volume of the polymer matrix.[26] For large molecules, however, the free volume in the polymer layer is not sufficient to accommodate the molecules. Therefore, the diffusion of the large molecules is only possible through the consecutive wriggling of the polymer chains. The free volume in polymer layers is directly proportional to the water uptake. The small dye molecules can diffuse out along the water path when the swelling of polymer films is considerable. Even when the water swelling is not sufficient, water molecules act as a plasticizer to lower the modulus and enhance the motion of the polymer chains, thus inducing the increased diffusivity of solute molecules. Comparison of the diffusivity ratio with the slope ratio (release rate ratio) reveals that the solubility of rhodamine B in polymer membranes also contributes to the release behavior as explained in eqn (3) and (5). Fig. 7B shows the relative solubility ($C_p/C_{p,PS20k}$) of each polymer normalized by the solubility of PS(20k). The solubility of dye molecules in the PS-NTA layer was approximately 4.5 times larger than that in PS(20k). The solubility in the PS-*t*-Bu layer was 1.5-fold of that in the PS(20k) layer. This is well matched with the tendency of water uptake in each polymer shown in Fig. 5. High degree of water uptake in a polymer thin film increased both the diffusivity and solubility, but the degree of increase in the two characteristics should not be the same.

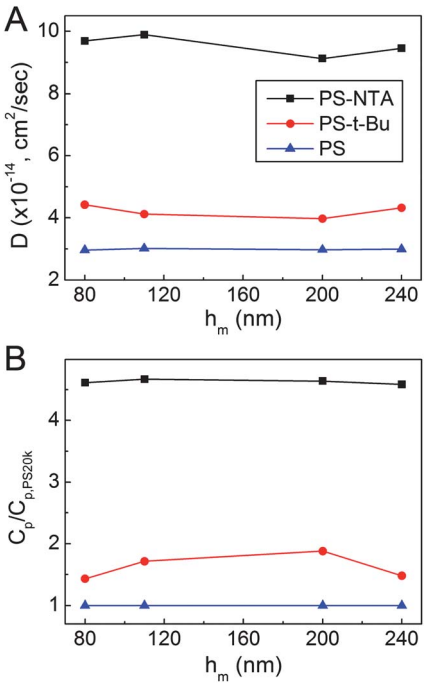

Fig. 7 (A) Diffusivity of rhodamine B in polymer membranes with different thicknesses and (B) the relative solubility ($C_p/C_{p,PS20k}$) of rhodamine B normalized by the value in the PS(20k) layer. The solid lines in each plot are simple guide to eyes.

As a model study for high-molecular-weight molecules such as proteins and polymers, the release of FITC-labeled dextran (M_w = 10 000) was investigated. Fig. 8 shows the release profiles of dextran through PS(20k), PS-*t*-Bu, and PS-NTA with 80 nm thickness. Regardless of polymer layers, the dextran molecules were not released. It is because the free volume within the polymers as well as the segmental motion of polymer chains is not enough to accommodate the dextran molecules, preventing the outward diffusion of the molecules.

Molecular release through the PS-NTA layers with hydrophobic surface treatment

Since water uptake of a polymer layer is critical to solubility and diffusion of solute molecules, the surface energy of the polymer

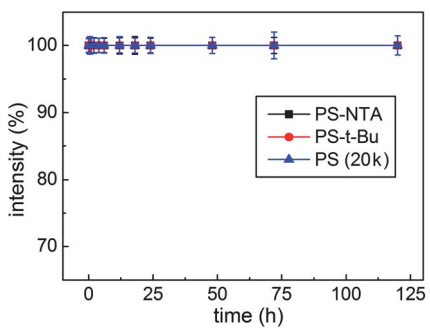

Fig. 8 Release behavior of fluorescent dextran through various polymer membranes with 80 nm thickness. Experimental symbols of (■), (●), and (▲) correspond to PS-NTA, PS-*t*-Bu, and PS(20k), respectively. Solid lines are simple guides to eyes. No molecules were released through the polymer layers.

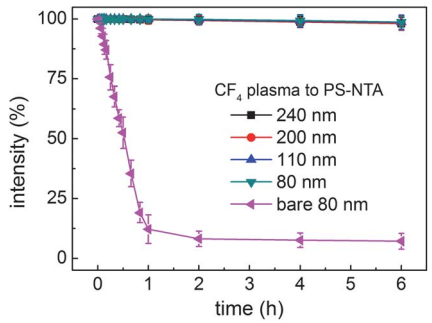

Fig. 9 Effect of CF_4 plasma treatment to the PS-NTA layer on the release behavior of rhodamine B.

layer can play an important role in the release of molecules. Simple surface treatment for hydrophilicity or hydrophobicity may significantly increase or decrease the release rate of molecules.[14] Fig. 9 shows the release profile of rhodamine B through CF_4 plasma-treated PS-NTA thin films. It is well established that CF_4 plasma effectively fluorinates polymer surfaces to turn them hydrophobic.[27] After the plasma treatment, the contact angle on the PS-NTA layer increased from 52° to 101° as shown in Fig. S3 in the ESI†. The release rate of rhodamine B was found to be much smaller than that without the plasma treatment (left triangle). The 80 nm thick bare PS-NTA without the plasma treatment allowed almost 100% release within 4 h for rhodamine B. Meanwhile, the plasma treated PS-NTA considerably deterred the release so that less than 2% rhodamine B was released in 6 h at any film thickness. This is because the prohibited water absorption in the fluorinated surface layer retarded the release of the molecules. The penetration depth of CF_4 plasma has been known to be a few nm depending on the operation condition and the material.[28] To quantify the effect of plasma on release behavior, eqn (3) was modified as a double layer model,[29]

$$\frac{Q}{t} = \frac{A C_f C_p D_f D_m}{h_f D_m C_p + h_m D_f C_f} \quad (7)$$

where h_f, C_f, and D_f are the thickness, solubility and diffusivity of molecules in the fluorinated surface layer. The plasma-treated layer was calculated to be 5 nm by using eqn (3) and (7). The calculated diffusivity for rhodamine B in the fluorinated layer was 1.43×10^{-15} cm^2 s^{-1}. The plasma treatment also affected the solubility of the solute molecules so that the normalized ratio by the untreated PS-NTA layer was 0.002.

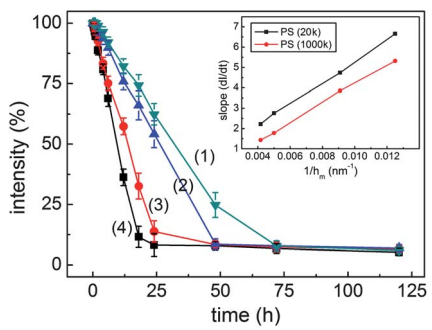

Fig. 10 Release behavior of rhodamine B through the high molecular weight PS(1000k) layers with different thicknesses: (1) 240 nm, (2) 200 nm, (3) 110 nm, and (4) 80 nm. The inset is the comparison of release rates with that through PS(20k).

Molecular release through the high-molecular-weight PS layers

The molecular weight of the membrane polymer can be a controllable factor for the diffusion as shown in eqn (3). Siepmaan *et al.* reported that release of the ophylline in ethyl cellulose slowed down as the chain length of ethyl cellulose was increased.[30] Longer polymer chains increase entanglement of the chains, leading to smaller free volume and decreasing the movement of the polymer chains. In this study, the release through the layer of long-chain PS matrix, PS(1000k), was compared with the results in PS(20k). Fig. 10 shows the release profile of rhodamine B through the PS(1000k) layer. The release of rhodamine B was similar to the results in PS(20k). The inset of Fig. 10 is a plot which compares the release rate (slope) in the steady-state region between PS(20k) and PS(1000k). The average diffusivity of rhodamine B in PS(1000k) was calculated to be 2.35×10^{-14} cm^2 s^{-1} and the diffusivity ratio of PS(20k) to PS(1000k) was coincident with the slope ratio of PS(20k) to PS(1000k). Overall, the results demonstrate that the release of small molecules through a long-chain matrix was slower than that through a short-chain matrix, but the effect of chain length of the diffusion barrier was not significant. This is because the water absorption in PS(20k) and PS(1000k) is comparable. Since small molecules such as rhodamine B do not need significant motions of the polymer chains for their diffusion, hydration compensates for the decreased polymeric free volume in the PS(1000k) layer.

4. Conclusion

We have developed a novel method to monitor molecular release through thin polymer barriers by employing the buckling of polymer thin films to fabricate uniform and submicron-sized molecular reservoirs. The method allows systematic studies on molecular release by adjusting various parameters in

Table 1 Summary of the diffusion-related data: swelling, release rate, diffusion, and relative solubility

		PS(20k)	PS-*t*-Bu(18k)	PS-NTA(15k)	Fluorinated PS-NTA(15k)[d]	PS(1000k)
Volume increase by hydration[a]		1.04	1.06	1.13	1.03	1.03
Rhodamine B	Release rate (%/h)	2.22	4.74	32.15	0.3	1.44
	Diffusivity[b]	2.52×10^{-14}	4.32×10^{-14}	9.45×10^{-14}	1.34×10^{-15}	2.35×10^{-14}
	Relative solubility ($C_p/C_{p,PS20k}$)[c]	1	1.43	4.18	0.01	0.92

[a] The film thickness was fixed at 240 nm. [b] The unit is cm^2 s^{-1}. [c] Normalized by the solubility in the PS(20k) film. [d] Calculated diffusivities and solubilities are values of the fluorinated surface layer, not whole film.

the polymer barriers such as polymer species, molecular weight, thickness, and surface energy. Simple analysis of the release profile gives information of diffusivity and relative solubility of the solute molecules in the polymeric barriers. Furthermore, the easy deposition of various molecules facilitates the study of the difference in molecular release according to the molecular species. As a model study, we chose rhodamine B and FITC-labeled dextran polymer to represent small drugs and large drugs. We theoretically analyzed their release behavior according to degree of hydration, thickness, surface energy, and molecular weight of the barrier polymers. The results are summarized in Table 1. The degree of water uptake was controlled by changing the chain end group of PS to *tert*-butyl (PS-*t*-Bu) and nitrilotriacetic acid (PS-NTA). The NTA-terminated PS thin films showed 13% water absorption regardless of the film thickness and exhibited fast molecular release for small molecules. On the other hand, the bare PS and the *t*-Bu-terminated PS barriers exhibited 4% and 6% hydration and showed a slow release behavior for small molecules. It turned out that increased hydration raises both the diffusivity and solubility of the solute molecules in the polymer barriers. Release of small molecules was not dependent on the molecular weight of the barrier polymers. For large molecules, the release was blocked due to the restricted accommodation by the polymer chains of the barrier layer. Surface treatment by CF_4 plasma on the PS-NTA barriers considerably retarded the release of small molecules. This method will be utilized to investigate more details of release dependence on the shape, interaction, structure, and mass of various target molecules through solid or porous polymeric barriers. Further, fabrication of multilayer barriers can be used to model complex delivery systems in the future.

Acknowledgements

We would like to acknowledge the financial support from the National Research Foundation (NRF) grant funded by the Korean Government (MEST) through the Active Polymer Center Pattern Integration (R11-2007-050-01004-0) and the World Class University (WCU) Program (R32-20031).

References

1 (*a*) A. Paiva, M. D. Foster and E. D. V. Meerwall, *J. Polym. Sci., Part B: Polym. Phys.*, 1998, **36**, 373; (*b*) H. Kato, S. Takemura and Y. Nakajima, *Thin Solid Films*, 1998, **317**, 367; (*c*) I. Krögel and R. Bodmeier, *J. Controlled Release*, 1999, **61**, 43; (*d*) C. Anandan, J. B. Bharathibai and K. S. Rajam, *Eur. Polym. J.*, 2004, **40**, 1833; (*e*) R. Suedee, C. Bodhibukkana, N. Tangthong, C. Amnuaikit, S. Kaewnopparat and T. Srichana, *J. Controlled Release*, 2008, **129**, 170.

2 (*a*) H. Yang and W. J. Ooij, *Plasmas Polym.*, 2003, **8**, 297; (*b*) F. Faÿ, I. Linossier, J. J. Peron, V. Langlois and K. Vallée-Rehel, *Prog. Org. Coat.*, 2007, **60**, 194; (*c*) E. Jo, S. Lee, K. T. Kim, Y. S. Won, H. S. Kim, E. C. Cho and U. Jeong, *Adv. Mater.*, 2008, **21**, 968; (*d*) S. H. Hu, S. Y. Chen, D. M. Liu and C. S. Hsiao, *Adv. Mater.*, 2008, **20**, 2690; (*e*) K. Katagiri, K. Koumoto, S. Iseya, M. Sakai, A. Matsuda and F. Caruso, *Chem. Mater.*, 2009, **21**, 195; (*f*) R. Wang, R. P. Moody, D. Koniecki and J. Zhu, *Environ. Int.*, 2009, **35**, 900.

3 Y. C. Dong and S. S. Feng, *J. Biomed. Mater. Res., Part A*, 2006, **78**, 12.

4 M. Polakovic, T. Görner, R. Gref and E. Dellacherie, *J. Controlled Release*, 1999, **60**, 169.

5 A. Halder and B. Sa, *AAPS PharmSciTech*, 2006, **7**, E46.

6 K. W. Leong and R. Langer, *Adv. Drug Delivery Rev.*, 1987, **1**, 199.

7 (*a*) S. Akerman, P. Viinikka, B. Svarfvar, K. Jarvinen, K. Kontturi, J. Nasman, A. Urtti and P. Paronen, *J. Controlled Release*, 1998, **50**, 153; (*b*) L. Vaccari, D. Canton, N. Zaffaroni, R. Villa, M. Tormen and E. di Fabrizio, *Microelectron. Eng.*, 2006, **83**, 1598; (*c*) E. J. Anglin, L. Y. Cheng, W. R. Freeman and M. J. Sailor, *Adv. Drug Delivery Rev.*, 2008, **60**, 1266.

8 (*a*) W. W. Brandt, *J. Phys. Chem.*, 1959, **63**, 1080; (*b*) Y. W. Chien, *Novel Drug Delivery Systems*, Dekker, New York, 2nd edn, 1992, ch. 2; (*c*) M. Grassi and I. Colombo, *J. Controlled Release*, 1999, **59**, 343.

9 (*a*) G. Huang, J. Gao, Z. Hu, J. V. St. John, B. C. Ponder and D. Moro, *J. Controlled Release*, 2004, **94**, 303; (*b*) B. J. Boyd, *Expert Opin. Drug Delivery*, 2008, **5**, 69; (*c*) A. F. Azarbayjani, A. Jouyban and S. Y. Chan, *J. Pharm. Pharm. Sci.*, 2009, **12**, 218.

10 D. Y. Arifin, L. Y. Lee and C. H. Wang, *Adv. Drug Delivery Rev.*, 2006, **58**, 1274.

11 (*a*) N. Bowden, S. Brittain, A. G. Evans, J. W. Hutchinson and G. M. Whitesides, *Nature*, 1998, **393**, 146; (*b*) J. Y. Chung, A. J. Nolte and C. M. Stafford, *Adv. Mater.*, 2011, **8**, 349.

12 (*a*) D. S. Gray, J. Tien and C. S. Ghen, *Adv. Mater.*, 2004, **16**, 393; (*b*) D. Y. Khang, H. Jiang, Y. Huang and J. A. Rogers, *Science*, 2006, **311**, 208; (*c*) S. Béfahy, S. Yunus, T. Pardoen and P. Bertrand, *Appl. Phys. Lett.*, 2007, **91**, 141911.

13 (*a*) C. M. Stafford, C. Harrison, K. L. Beers, A. Karim, E. J. Amis, M. R. Vanlandingham, H. C. Kim, W. Volksen, R. D. Miller and E. E. Simonyi, *Nat. Mater.*, 2004, **3**, 545; (*b*) A. J. Nolte, M. F. Rubner and R. E. Cohen, *Macromolecules*, 2005, **38**, 5367; (*c*) C. M. Stafford, S. Guo, C. Harrison and Y. M. Chiang, *Rev. Sci. Instrum.*, 2005, **76**, 062207; (*d*) A. J. Nolte, R. E. Cohen and M. F. Rubner, *Macromolecules*, 2006, **39**, 4841; (*e*) E. A. Wilder, S. L. Guo, M. J. Gibson, M. J. Fasolka and C. M. Stafford, *Macromolecules*, 2006, **39**, 4138.

14 D. C. Hyun, G. D. Moon, C. J. Park, B. S. Kim, Y. Xia and U. Jeong, *Angew. Chem., Int. Ed.*, 2011, **50**, 724.

15 (*a*) D. C. Hyun, G. D. Moon, C. J. Park, B. S. Kim, Y. Xia and U. Jeong, *Adv. Mater.*, 2010, **22**, 2642; (*b*) D. C. Hyun, M. Park, C. J. Park, B. S. Kim, Y. Xia, J. H. Hur, J. J. Park and U. Jeong, *Adv. Mater.*, 2011, **23**, 2946.

16 H. Y. Cho, M. A. Kadir, B. S. Kim, H. S. Han, S. Nagasundarapandian, Y. R. Kim, S. B. Ko, S. G. Lee and H. Paik, *Macromolecules*, 2011, **44**, 4672.

17 M. Morra, E. Occhiello, R. Marola, F. Garbassi, P. Humphrey and D. Johnson, *J. Colloid Interface Sci.*, 1990, **137**, 11.

18 D. C. Hyun and U. Jeong, *J. Appl. Polym. Sci.*, 2009, **112**, 2683.

19 H. Jiang, D. Y. Khang, J. Song, Y. Sun, Y. Huang and J. A. Rogers, *Proc. Natl. Acad. Sci. U. S. A.*, 2007, **104**, 15607.

20 C. T. Koh, Z. J. Liu, D. Y. Khang, J. Song, C. Lu, Y. Huang, J. A. Rogers and C. G. Koh, *Appl. Phys. Lett.*, 2007, **91**, 133113.

21 J. Crank, *The Mechanics of Diffusion*, Clarendon Press, Oxford, 2nd edn, 1975.

22 Y. W. Chien, *Sustained and Controlled Release Drug Delivery System*, ed. J. R. Robinson, Dekker, New York, 1978, ch. 4.

23 (*a*) I. Linossier, F. Gaillard, M. Romand and J. F. Feller, *J. Appl. Polym. Sci.*, 1997, **66**, 2465; (*b*) S. I. Ahn, J. G. Yoon, J. H. Kim and W. C. Zin, *Langmuir*, 2010, **26**, 18483.

24 (*a*) G. M. Zentner, J. R. Cardinal and S. W. Kim, *J. Pharm. Sci.*, 1978, **67**, 1347; (*b*) G. M. Zentner, J. R. Cardinal and S. W. Kim, *J. Pharm. Sci.*, 1978, **67**, 1352.

25 (*a*) Z. J. Zhao, Q. Wang and L. Zhang, *J. Phys. Chem. B*, 2007, **111**, 4411; (*b*) Z. J. Zhao, Q. Wang and L. Zhang, *J. Phys. Chem. B*, 2007, **111**, 13167.

26 (*a*) Y. Tamai, H. Tanaka and K. Nakanishi, *Macromolecules*, 1994, **27**, 4498; (*b*) Y. Tamai, H. Tanaka and K. Nakanishi, *Macromolecules*, 1995, **28**, 2544; (*c*) Y. Tamai, H. Tanaka and K. Nakanishi, *Macromolecules*, 1995, **104**, 363.

27 K. Endo and T. Tatsumi, *J. Vac. Sci. Technol., A*, 1991, **9**, 2948.

28 J. Meichsner, *Contrib. Plasma Phys.*, 1999, **39**, 427.

29 K. Tojo, C. C. Chiang and Y. W. Chien, *J. Pharm. Sci.*, 1987, **76**, 123.

30 J. Siepmann, F. Lecomte and R. Bodmeier, *J. Controlled Release*, 1999, **60**, 379.

